Accepted Manuscript

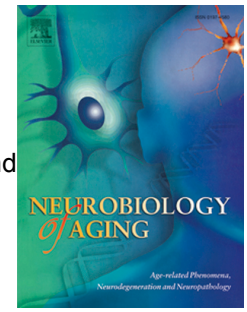

The segregated connectome of late life depression: a combined cortical thickness and structural covariance analysis

E. Mak, S.J. Colloby, A. Thomas, J.T. O'Brien

PII: S0197-4580(16)30191-9

DOI: 10.1016/j.neurobiolaging.2016.08.013

Reference: NBA 9699

To appear in: *Neurobiology of Aging*

Received Date: 24 April 2016

Revised Date: 2 August 2016

Accepted Date: 13 August 2016

Please cite this article as: Mak, E, Colloby, S., Thomas, A, O'Brien, J., The segregated connectome of late life depression: a combined cortical thickness and structural covariance analysis, *Neurobiology of Aging* (2016), doi: 10.1016/j.neurobiolaging.2016.08.013.

The segregated connectome of late life depression: a combined cortical thickness and structural covariance analysis

Mak E [1], Colloby SJ [2], Thomas A [2], O'Brien JT [1].

[1] Department of Psychiatry, University of Cambridge, UK., [2] Institute of Neuroscience, Newcastle University, Newcastle, UK.

Corresponding author:
Professor John O'Brien
Foundation Professor of Old Age Psychiatry
Department of Psychiatry
University of Cambridge School of Clinical Medicine
Box 189, Level E4 Cambridge Biomedical Campus
Cambridge
CB2 0SP
UK

Word count: 4449
Abstract: 185
Figures and tables: 7
Running title: Segregated brain networks in late-life depression

Keywords: imaging;depression;dementia;graph theory;brain network;late-life depression;psychiatry

ABSTRACT

Late-life depression (LLD) has been associated with both generalized and focal neuroanatomical changes including grey matter atrophy and white matter abnormalities. However, previous literature has not been consistent and, in particular, its impact on the topology organisation of brain networks remains to be established. In this multi-modal study, we first examined cortical thickness, and applied graph theory to investigate structural covariance networks in LLD. 33 subjects with LLD and 25 controls underwent T1-weighted, fluid attenuated inversion recovery (FLAIR) and clinical assessments. Freesurfer was used to perform vertex-wise comparisons of cortical thickness, while the Graph Analysis Toolbox (GAT) was implemented to construct and analyze the structural covariance networks. LLD showed a trend of lower thickness in the left insular region ($p<0.001$ uncorrected). In addition, the structural network of LLD was characterised by greater segregation, particularly showing higher transitivity (i.e. measure of clustering) and modularity (i.e. tendency for a network to be organised into sub-networks). It was also less robust against random failure and targeted attacks. Despite relative cortical preservation, the topology of the LLD network showed significant changes particularly in segregation. These findings demonstrate the potential for graph theoretical approaches to complement conventional structural imaging analyses and provide novel insights into the heterogeneous aetiology and pathogenesis of LLD.

INTRODUCTION

Late-life depression (LLD), often defined as depression in people over the age of 60, is common, and often associated with cognitive decline and future risk of dementia, increased disability, and mortality (Naismith et al., 2012). Estimates of the prevalence of clinically relevant depressive symptoms in older adults typically range from 10-15% and rates of major depression from 1-5%. Several diverse etiological factors have been proposed, including structural abnormalities due to vascular (Thomas et al., 2001) and neurodegenerative factors (Tsopelas et al., 2011), hypothalamo-pituitary-adrenal axis dysfunction and dysregulation of neurotransmitters such as serotonin (Meltzer et al., 1998).

Previous imaging studies have revealed a varied assortment of structural and functional abnormalities: localised grey matter atrophy in frontal cortex (Ballmaier et al., 2004) and subcortical structures (Colloby et al., 2011c), increased distribution of white matter hyperintensities (WMH) (Herrmann et al., 2007), microstructural deficits in white matter pathways (Sexton et al., 2015), and altered functional connectivity between subcortical regions (Kenny et al., 2010). However, the prevailing neuroimaging literature in LLD is still inconclusive. A meta-analysis of MRI studies in LLD only found weak evidence of hippocampal atrophy (7 out of 15 studies) (Sexton et al., 2013), while others have not demonstrated any significant differences in grey matter (Colloby et al., 2011b; Koolschijn et al., 2010) or WMH (Colloby et al., 2011c). A previous hypothesis-driven comparison of frontal lobar cortical thickness in this sample also did not show any significant differences compared to healthy controls (Colloby et al., 2011b). These disparate findings could simply reflect the heterogeneity and the complex interaction of various factors in the pathophysiology of LLD, which might in turn obscure subtle disease-related alterations in the interaction patterns existing in large-scale networks of brain regions. In this regard, a multivariate technique might better explain the reported variability in neuroanatomical findings across studies

compared to the conventional approach examining localised differences in discrete regions between groups.

In recent years, graph theoretical concepts have been increasingly applied to study the organisational principles of the brain by modelling it as a large-scale network with interconnected nodes and edges (Bullmore and Sporns, 2009). This framework rests on the fundamental premise that the maintenance or disintegration of complex systems is shaped by the interactions among their constituent elements. Bearing similarities to real-world scenarios such as the social-network (i.e. six degrees of separation) and the cascading hyperlinks of the Internet, the human brain also possesses an inherent architecture known as the "small-world phenomenon" (Hagmann et al., 2008; Sporns et al., 2005). The small-world topology, with its short path lengths and high clustering (see Table 1 for a brief description of each network measure), supports efficient segregation and distribution of information processing with minimal cost (Bullmore and Sporns, 2009), and confers resilience against pathological damage (Achard et al., 2006). Conversely, deviations from small-worldness towards randomisation (shorter path lengths and lower clustering) or regularisation (longer path lengths and higher clustering) have been found in the networks associated with neurodegenerative and psychiatric diseases, such as Alzheimer's disease (He et al., 2008), schizophrenia (Bassett et al., 2008), and major depressive disorder (Singh et al., 2013). The structural covariance method, referring to the coordinated variations in grey matter morphology (e.g. cortical thickness or volume), is increasingly used to infer structural connectivity between regions and construct large-scale brain networks (Alexander-Bloch et al., 2013). A key assumption underlying this methodology is that morphological correlations are related to some degree of axonal connectivity between brain regions with shared trophic, genetic, and neurodevelopmental influences (Alexander-Bloch et al., 2013). Although altered structural covariance networks have been found in a variety of brain diseases, it remains challenging to interpret disease-related changes in networks as we

presently lack a clear understanding of the cellular and molecular mechanisms that drive the emergence of large-scale covariance across networks. Nevertheless, structural covariance networks derived from cortical thickness correlations have shown substantial agreement with white matter connections (Gong et al., 2012) and functional connectivity (Kelly et al., 2012).

To date, there have been very few studies assessing large-scale networks in LLD, yielding inconclusive evidence (See Table 2 for a literature summary). A recent diffusion tensor imaging (DTI) study of white matter connections identified longer path length and impaired global efficiency in LLD compared to controls (Bai et al., 2012). Using inter-regional correlations of grey matter volumes, another study in LLD also reported higher clustering in addition to longer path length (Ajilore et al., 2014), although no network differences were revealed by the same group in a subsequent analysis of white matter network on the same sample (Charlton et al., 2014). Preserved network organisation in LLD has been reported in other studies using grey matter volumes (Lim et al., 2013) and functional data (Bohr et al., 2013). Furthermore, no study has performed a combined analysis of regional cortical thickness and network properties in the same sample, which will allow us to directly investigate the macro-level impact of cortical atrophy beyond the potentially affected regions.

The aims of this multi-modal study are threefold: (a) we extended our previous frontal lobe study on this sample by employing a whole-brain vertex-wise approach to compare cortical thickness between LLD and controls; (b) from the regional thickness measures across the whole brain, we constructed a structural covariance network from the inter-regional correlations of cortical thickness to investigate global and regional properties of the LLD network; (c) and lastly, we investigated the resilience of both networks against random failures and targeted attacks. We hypothesized that LLD

would be characterised by lower regional cortical thickness as well as aberrations in small-worldness reflecting a shift towards a regularisation of the network.

METHOD

Participants and clinical assessment

Subjects above the age of 60 presenting to local psychiatry services with a history of a major depressive episode (DSM-IV criteria), current or previous were recruited. Specifically, the LLD group comprised of participants who were still depressed (n=16) as well as others who had remitted (n=17). Healthy individuals were recruited via an advertisement placed in the local Elders Council magazine inviting participation to the study and all came from the same geographical area as the participants with depression. All participants and controls underwent the same set of assessments and structured interviews, although the controls did not do the mood rating scale. Thus, only healthy controls without a history of serious medical disorders such as stroke, diabetes, cancer, or other neurological diseases were recruited. Participants in the depression group were required to fulfill DSM-IV criteria for a lifetime diagnosis of major depressive episode.

A full neuropsychiatric assessment was conducted including family history of depression, previous psychiatric history, medical history and current medication. Depression severity was rated using the Montgomery-Asberg Depressing Rating Scale (MADRS) (Montgomery and Asberg, 1979) and the 30-item Geriatric Depression Scale (GDS) (Yesavage et al., 1982). For all participants, the following exclusion criteria applied: dementia or MMSE score below 24, current use of a tricyclic antidepressant; comorbid or previous drug or alcohol misuse; previous head injury; previous history of epilepsy; previous transient ischaemic attack or stroke; or a myocardial infarction within the previous 3 months.

Standard protocol approvals, registrations, and patient consents

The study was approved by the Newcastle and North Tyneside Research Ethics Committee. All subjects provided written informed consent.

MRI acquisitions: T1, FLAIR, and DTI

Structural T1 imaging was performed a 3T Achieva MR scanner (Philips Medical Systems, Eindhoven, The Netherlands). The T1 weighted volumetric sequence covered the whole brain (MPRAGE, sagittal acquisition, slice thickness = 1.2 mm, voxel size = 1.15 x 1.15 mm; repetition time (TR) = 9.6 ms; echo time (TE) = 4.6 ms; flip angle = 8°; SENSE factor =2). The FLAIR sequence was as follows: TR = 11000ms, TE = 125ms, inversion time (TI)= 2800ms, SENSE factor = 1.5, voxel size = 1.02 mm x 1.02 mm, 60 slices, slice thickness = 2.5 mm.

Image preprocessing

Estimating cortical thickness from T1 MRI

Cortical reconstruction and volumetric segmentation of MRI data were performed using the Freesurfer image analysis suite (http://surfer.nmr.mgh.harvard.edu/) (Fischl and Dale, 2000; Fischl et al., 1999). The initial processing of T1 MRI images, for each subject and each time point (baseline and follow-up), includes the following steps: removal of non-brain tissue, automated Talairach transformation, segmentation of the subcortical white matter and deep grey matter volumetric structures, intensity normalization, tessellation of the grey matter/white matter boundary, automated topology correction and surface deformation to optimally place the grey matter/white matter and grey matter/CSF boundaries. The cortical thickness was calculated as the closest distance from the grey/white matter boundary to the grey/CSF boundary at each vertex. The cortical thickness maps were smoothed using a 10 mm full width half maximum Gaussian. All surface models in our study were visually inspected for accuracy and manual corrections were

performed in the event of tissue misclassification/white matter errors while blinded to diagnostic group information. 10 subjects (5 controls and 5 LLD subjects) who had excessive pial or white matter surface segmentation errors after the manual correction were excluded from the analyses. Thus, the final sample was 25 controls and 33 LLD. To define the nodes for subsequent network analyses, the cortical thickness map of the cerebral cortex was parcellated using the Desikan-Killiany atlas, resulting in 34 regions of interest (ROI) for each hemisphere, each corresponding to the average cortical thicknesses of a grey matter region (Desikan et al., 2006).

Quantifying white matter hyperintensities

Volumetric measurements of global, periventricular, and deep WMH were obtained for each subject using a previously validated method. The technical details of this have been previously described (Colloby et al., 2011c).

Vertex-wise comparisons of cortical thickness

Differences in regional cortical thickness between groups were assessed using a vertex-wise General Linear Model (GLM) in Freesurfer QDEC. The model included cortical thickness as a dependent factor and diagnostic group (LLD and controls) as an independent factor. Age, gender, and Cumulative illness rating scale for geriatrics (CIRS-G) were included as nuisance covariates. Correction for multiple comparisons was performed using False Discovery Rate (FDR) with significance threshold set at $p < 0.05$.

Structural covariance analyses

Defining the nodes using inter-regional correlations of cortical thickness

The full pipeline for the network analyses is illustrated in Figure 1. To investigate the alterations in the architecture of structural networks in LLD compared to controls, we applied graph theoretical

methods using the Graph Analysis Toolbox (Hosseini et al., 2012), which integrates the Brain Connectivity Toolbox (Rubinov and Sporns, 2010) for the calculation and statistical comparisons of network measures. Specifically, networks were constructed for the LLD and control group using the structural covariance approach (Alexander-Bloch et al., 2013). The nodes in the network correspond to the 68 cortical ROIs extracted from the Desikan-Killiany atlas. Consistent with previous studies, linear regression was performed at each ROI to remove the effects of covariates, including age, gender, CIRS-G, and mean cortical thickness (Bernhardt et al., 2011; He et al., 2007). The resulting residuals of this regression are then substituted for the unadjusted cortical thickness at each ROI. Therefore, the structural covariance networks for the LLD and controls group were constructed based on a 68 x 68 association matrix, with each entry defined as the Pearson correlation coefficient *R* between every pair of ROI.

Defining the edges through thresholding

From the association matrix for each group, a binary matrix is derived after thresholding, where an entry is 1 if *R* is greater than a minimum density threshold in each group. Consistent with previous studies (Hosseini et al., 2012; Pereira et al., 2016), we thresholded the association matrices at a range of network densities, from a minimum density of 10% to 20% in steps of 1%. This was done to ensure that group differences are not confounded by differing number of nodes and edges due to an absolute threshold at a single density. The density of a network relates to the fraction of edges present in the network compared to the maximum possible number of edges. The minimum density (D_{min}) is the density at which all the nodes are fully connected in the network of each group. This ensures that none of the networks are fragmented. The diagonal elements of the association matrix (i.e. self-connections) are set to zero. The resultant adjacency matrix represents a binary undirected graph. After generating the structural covariance networks of LLD and controls, we compared the network measures of interest across the range of densities. These measures include small-

worldness, characteristic path length, global efficiency, clustering coefficient, local efficiency, transitivity, and modularity. Brief descriptions of the network measures in this study are provided (Table 1).

Statistical comparisons of network measures between LLD and controls

The binarised adjacency matrices are then estimated by applying the same thresholding procedure as described above. To test the statistical significance of the between-group differences in network measures, non-parametric permutation tests with 1000 repetitions were performed in GAT. In conjunction with permutation testing, area under a curve (AUC) analyses was implemented to compare the curves depicting changes in a specific network measure (for each group) as a function of network density (Hosseini et al., 2012). Each of these curves depicts the changes in a specific network measure as a function of network density. The significance of the between-group differences in the AUC of each measure was similarly tested with a permutation analysis as described (Hosseini et al., 2012). A key advantage of this secondary approach is that by providing a summary *p* value of difference, the comparison between network measures is less sensitive to the thresholding process.

Investigating network resilience to random failure and targeted attacks

To assess the resilience of brain networks in LLD and controls to acute and focal damage, networks can be lesioned by random deletions of nodes or by targeted attack based on the highest degree or clustering of a node (Achard et al., 2006; Joyce et al., 2013; Váša et al., 2015). Random failure of the networks was simulated by randomly removing one node from the network. The impacts of these computational insults in both LLD and control networks were quantified by measuring the relative changes in the size of the largest remaining component. The largest remaining component

in a network refers to a sub-graph in which any two vertices are connected via edges, and which is not connected to the rest of the graph. To assess the network behaviour against targeted attacks, the same procedure was applied by removing nodes in rank order of decreasing betweenness centrality, a measure of the number of the shortest paths that pass through one node. The removal of nodes on the basis of betweenness centrality is a suitable paradigm for the assessment of network robustness because it characterises the relative influence of a brain region / node for integration of information across multiple brain regions. Finally, to test the differential responses of the networks in each group against random failure and targeted attacks, a permutation analysis was performed as previously described. The comparisons of network resilience were made at D_{min}, the lowest density at which all regions were fully connected in both networks. This ensured the involvement of all regions in the network model without extraneous connections that could confound the results of subsequent network failure analyses.

Qualitative hub analyses

We also performed a descriptive analysis of the spatial distribution of hubs in the networks of controls and LLD. Hubs are crucial components for efficient communication in a network as they are usually traversed by a large number of shortest paths between pairs of nodes (Bullmore and Sporns, 2009). In healthy controls, hubs have been found within highly connected association cortex while previous studies have also found altered distribution of hubs in neurodegenerative conditions such as AD (He et al., 2008). A region or node is considered a hub if its betweenness centrality is 2 SD greater compared to the network.

Statistical analyses

Statistical analyses were performed with the STATA13 (http://www.stata.com/) software. Distribution of continuous variables was tested for normality using the Skewness-Kurtosis test and

visual inspection of histograms. Parametric data was assessed using either t-tests or analysis of variance (ANOVA) for continuous variables. For non-parametric data, Wilcoxon rank-sum test or Kruskal-Wallis test was used. χ^2 tests were used to examine differences between categorical variables. ANCOVA was used to compare the distribution of WMH, accounting for age, gender and intracranial volumes. For each test statistic, a two-tailed probability value of < 0.05 was regarded as significant.

RESULTS

Sample characteristics and clinical features

Demographics, clinical characteristics and imaging measures of the sample are shown in Table 3. Both the LLD group and controls were well matched for age (p=0.960) and gender (p=0.746). As might be expected, the LLD group scored significantly lower on MMSE (p=0.006), although both were within the normal range. 17 LLD subjects were in remission. There was no significant age (p=0.326) or gender (p=0.362) difference between those in remission compared to those who were not in remission. As expected, GDS scores were lower in the remission group (p<0.001). 17 subjects had early-onset depression. No differences in age (p=0.135), gender (p=0.362) and GDS (p=0.793) were found between early-onset and late-onset groups. The LLD group also had significantly higher CIRS-G scores, but this was due mainly to differences in genitourinary symptoms (p<0.001).

Cortical thickness comparisons

Global cortical thickness did not significantly differ between LLD and controls (p=0.341) (Table 3). Similarly, the vertex-wise comparisons with correction for multiple comparisons of cortical thickness found no differences between both groups. However, at a liberal threshold of $p < 0.001$

(uncorrected), the LLD group showed a focal reduction of cortical thickness in the left insular compared to healthy controls (Figure 2).

White matter hyperintensities comparisons

No differences were found between LLD and controls in all measures of WMH, including total WMH (p= 0.730), periventricular WMH (p= 0.991), and deep WMH (p= 0.534) (Table 3).

Structural covariance network analyses

The minimum density below which the networks in both groups were fragmented was D_{min} = 0.1. The networks of both groups showed small-world organisation across a wide range of densities (small world index > 1); suggesting that both networks had a path length slightly higher than random networks, while having a clustering coefficient much higher than that of a random network. We investigated between-group differences in global network measures on networks thresholded across a range of densities (0.1:0.01:0.2) (Figure 3). Although the LLD group showed longer lambda values (normalized characteristic path length) and lower global efficiency, this different was not significant across the range of network densities. However, the LLD network had significantly greater transitivity and modularity across the range of network densities. A subsequent AUC analysis consistently showed higher transitivity (p=0.025) and modularity (p=0.022).

Regional network characteristics

We investigated both the networks (density = 0.1) for between-group differences in regional network measures, such as nodal betweenness, nodal clustering, and nodal degree. No significant differences in nodal characteristics were found after correction for multiple comparisons across the 68 ROIs.

Network resilience against random failure and targeted attacks

Compared to the controls, the LLD network showed less tolerance to random failures (i.e. smaller size of the largest remaining component) at most fractions of removed node (Figure 4). To a smaller extent, the LLD network was also more vulnerable to targeted attacks by removal of nodes in rank order of decreasing betweenness centrality, showing significant fragmentation at 0.4 fraction of node removal. The LLD network was still more vulnerable to random failure after accounting for WMH as an additional covariate, whereas the between-group difference in robustness to targeted attacks was attenuated, and no longer significant.

Identification of hubs

The illustration of hubs in both groups is shown in Figure 5. In the networks thresholded at D_{min}, we considered a node a hub if its betweenness centrality is 2SD higher than the mean betweenness centrality in the network (He et al., 2008). The hubs in the control network were found in the left paracentral gyrus, right isthmus cingulate cortex, right rostral anterior cingulate cortex and right rostral middle frontal cortex. In the LLD network, only the right caudal anterior cingulate cortex was identified as a hub.

DISCUSSION

This was the first study to perform a combined analysis of regional cortical thickness and large-scale network properties in LLD. Our findings were partially consistent with our primary hypotheses. Despite showing a relative cortical preservation, the LLD network was characterised by higher segregation as reflected by greater transitivity and modularity compared to controls. This deviation from an optimal small-world architecture was also accompanied by lower resilience to random failure and targeted attacks, the latter of which could be partially mediated by WMH. These

results collectively suggest an altered topology of structural covariance networks in patients with LLD.

Previous ROI and voxel-based morphometry analyses on this sample by our group have demonstrated preserved frontal lobar cortical thickness and grey matter volumes respectively (Colloby *et al.*, 2011). The present study extended the analyses to perform a whole-brain, vertex-wise comparison of regional cortical thickness, and no significant reductions of cortical thickness were found in LLD. Although this observation sits in contrast to a meta-analysis revealing widespread grey matter reductions in LLD (Sexton et al., 2013), our negative finding is consistent with a previous study comparing 28 female subjects with LLD with 38 age-matched controls (Koolschijn et al., 2010). The relative absence of focal grey matter abnormalities has prompted us to argue that white matter pathology could be more pertinent to the neurobiology of LLD. Indeed, a previous DTI-Tract Based Spatial Statistics (TBSS) analysis on the same sample suggested subtle deficits of integrity in white matter fibers within frontal, temporal, and midbrain regions (Colloby *et al.*, 2011). In addition to microstructural alterations in white matter, the pathophysiological background of LLD is complicated by a host of factors, including vascular, neurotransmitter disruptions, and amyloidosis reminiscent of Alzheimer's disease pathology (Nascimento et al., 2015). Collectively, the broad range of changes in LLD has given rise to the notion that LLD could be characterised as a systems-level disorder, one that is particularly suited to be investigated by a multivariate network approach that considers the orchestrated interactions between distinct neuroanatomical regions.

In this study, the structural networks in LLD and controls were characterised by a small-world architecture that was not significantly different between groups. However, the small-worldness of a brain network is determined by its underlying attributes such as segregation and integration.

Although the LLD network showed longer characteristic path length and lower global efficiency, this difference did not reach statistical significance. A similar non-significant trend for longer path lengths have been previously reported in another sample of LLD (Ajilore et al., 2014), in addition to other significant findings of network disintegration has been reported in other studies of LLD (Bai et al., 2012; Li et al., 2014) and AD (Dai and He, 2014; He et al., 2008). On the other hand, segregation reflects the capacity to perform specialised processing within a clique of densely interconnected brain regions. The LLD network in the present study had greater transitivity and a higher degree of modularity, both of which have not been previously reported in the LLD graph theory literature (Table 2). The concept of modularity is increasingly popular in graph theory research, which posits that brain networks can be decomposed into classes of modules or sub-networks. As such, it is also another index for the degree to which the brain is compartmentalized. Indicative of an abnormally strong local specialization and segregation, our paired findings of higher transitivity and modularity could suggest that information processing in the LLD brain network is traversing restrictedly within a clique of densely interconnected regions.

However, in contrast to the well-established findings of lower integration in LLD, there is less agreement about the presence and direction of changes in the segregative properties of LLD networks: both higher (Ajilore et al., 2014) and lower (Li et al., 2014) clustering have been reported from structural and functional networks respectively. In parallel, a similar dichotomy of between-group differences in clustering has emerged in the AD graph theory literature, where structural and functional networks have demonstrated higher (Daianu et al., 2015; He et al., 2008; Yao et al., 2010) and lower (de Haan et al., 2009; Stam et al., 2009; Supekar et al., 2008) clustering respectively. The reconciliation of seemingly disparate findings from structural and functional networks represents a critical challenge in the rapidly growing field of graph theory, although it

could also serve to suggest that each imaging modality could be characterizing unique information about the human connectome albeit from different perspectives.

It is tempting to hypothesize that the segregated topology of the LLD network might render it less resilient to network dysfunction due to its failure to recruit alternative routes for information pathways (i.e. parallel processing) (Achard et al., 2006). In agreement with previous studies in LLD (Ajilore et al., 2014) and AD (He et al., 2008), both our findings support this hypothesis. The LLD networks showed a significantly greater degree of fragmentation when subjected to both random removal and targeted removals of nodes based on betweenness centrality. Considering the heterogeneous etiology of LLD, the potential involvement of vascular pathology to the weakened robustness of the LLD network was also investigated by accounting for WMH in a secondary analysis. While the LLD network was still showing less resilience to random attacks, between-group differences in robustness to targeted attacks were attenuated and no longer significant. This suggests that, instead of a diffuse effect of topological destabilization, WMH could be locally deleterious to highly influential nodes that serve as bridges between disparate components of a brain network. It would be desirable to test this hypothesis using single-subject connectivity matrices from resting-state functional MRI or diffusion tractography datasets.

There was a distinct distribution of hubs in both LLD and control networks. Specifically, a loss of hubs in frontal and posterior cortices was found in LLD compared to controls. LLD network showed which could, in turn, compromise the topological stability of the networks to both random and targeted attacks as described. Given their centrality to the networks, hubs are biologically costly and vulnerable to disease-related processes (Crossley et al., 2014). In this context, local blood flow of a node could represent a surrogate measure of ‘biological cost’. Indeed, hypoperfusion in frontal

regions is a consistent finding in LLD (Awata et al., 1998). Future studies are needed to further investigate the effects of hypoperfusion on network measures at the individual level.

With the repertoire of analyses across network measures, WMH-related network vulnerability and hub analyses, we could attempt to offer some tentative insights into the potential factors leading to the segregated adaptation of the LLD network observed in this study. Firstly, we have shown that WMH could account for network vulnerability against targeted attacks of nodes with high betweenness centrality, otherwise known as hubs. WMH and other ischemic changes are preferentially distributed within the periventricular and deep white matter regions, leading to disruptions of long projection fibers that are crucial for signal propagation across longer distances. The deletion of these 'network shortcuts' may induce a re-routing of network communications by forcing signal propagation to traverse neighboring and adjacent circuits, in turn increasing the segregation within the network. Secondly, the loss of frontal and posterior hubs in LLD could also lead to a fragmentation of the LLD network into dense clusters that are highly intra-connected but weakly inter-connected with other clusters of regions.

There are several strengths to our multi-modal study. To the best of our knowledge, this was the first study to compare regional cortical thickness and network measures in the same sample. Unlike the VBM approach in previous studies (Lim et al., 2013), we used regional cortical thickness to construct our structural covariance networks, thereby overcoming the main limitation of VBM: providing a mixed measure of the cortical gray matter, including surface area, cortical folding, as well as cortical thickness (Hutton et al., 2009). The structural covariance approach also offers another alternative approach that could sidestep the limited validity of DTI-based approaches to map cortico-cortical connectivity due to the multitude of branching and crisscrossing fibers. However, the structural covariance networks constructed in the current study is estimated on the

basis of inter-regional correlations at a group-level (LLD and controls) and does not provide individual networks for each subject, precluding correlational investigations with clinical measures, such as WMH burden as described previously. Our study also benefited from participants being clinically assessed by a psychiatrist. We used robust and validated methods for our imaging techniques, and the sample was reasonably sized compared with similar studies in late-life depression. A potential limitation was that we did not control for the potential effects of medication on the structural networks. It is possible that psychotropic medications could influence results but other medications typical in older populations such as anti-hypertensives and statins are less likely. However, since medications were too diverse in the depressed cohort, a rigorous statistical evaluation was impractical. Our ability to identify cortical changes might have been limited by the wide range of participants recruited, such as the grouping of LLD subjects both in remission and non-remission However, we believe our findings are generalisable in light of the heterogeneous nature of LLD (Ajilore et al., 2014). Furthermore, the Finally, although the number of graph metrics examined in this study was comparable to the literature, there could still be a risk of Type 1 error. Future studies with larger sample size are warranted to confirm our novel findings of higher transitivity and modularity in LLD networks. With regards to the image processing, 10 subjects were excluded due to segmentation errors that could not be adequately corrected. This is similar to other studies with a failure rate of 10-15% (Iscan et al., 2015; Watson et al., 2014). The performance of Freesurfer could be improved by averaging across multiple T1 scans per subject due to improvements in motion correction. This could be a consideration for future studies particularly in datasets involving elderly patients.

In this study, graph theoretical analyses revealed global network disruptions in LLD despite comparable cortical thickness to that of healthy controls. The LLD network was highly segregated with significantly higher transitivity and modularity, both of which have been consistently reported

in neurodegenerative conditions such as AD. These topological disruptions were accompanied by more vulnerability to network disturbances, which in turn, could be accounted by the presence of WMH. Taken together, these network disturbances provided early evidence that graph theory is a promising framework to investigate the heterogeneous aetiology and pathogenesis of LLD, although further studies in this growing field are warranted.

ACKNOWLEDGEMENTS

This work was supported by the NIHR Biomedical Research Unit in Dementia and the Biomedical Research Centre awarded to Cambridge University Hospitals NHS Foundation Trust and the University of Cambridge, and the NIHR Biomedical Research Unit in Dementia and the Biomedical Research Centre awarded to Newcastle upon Tyne Hospitals NHS Foundation Trust and the Newcastle University. Elijah Mak was in receipt of a Gates Cambridge, PhD studentship.

FINANCIAL DISCLOSURES

Elijah Mak has no competing interests.

Sean Colloby has no competing interests.

Alan Thomas reports grants from the Medical Research Council, NIHR, ARUK and the Alzheimer's Society and has received funding from GE Healthcare for investigator led research

John O'Brien reports grants from the Medical Research Council, NIHR, ARUK and the Alzheimer's Society and has acted as a consultant for GE Healthcare, Lilly, TauRx, Axona and Cytox.

TABLES AND FIGURES

Small worldness is a measure of how much a network is locally interconnected compared against a random network while retaining efficient global connectivity between distant brain regions. Thus, its main attributes are a higher clustering coefficient but a similar characteristic path length compared with that of a random network.			
Integration		**Segregation**	
Characteristic path length	The shortest path length is the smallest number of connections to get from one node to another. The characteristic path length is the average of the shortest path length between all the pairs of nodes in the network. It is the most commonly used measure of network integration.	Clustering coefficient	The clustering coefficient of a node is a measure of the number of edges that exist between its nearest neighbours. The clustering coefficient of a network is thus the average of clustering coefficients across the nodes.
Global efficiency	The global efficiency is the average of the inverse shortest path length in the network.	Transitivity	Often used as an alternative to clustering coefficient, transitivity reflects the likelihood for a network to have interconnected nodes that are adjacent to one another, and is normalized by the whole network. It is also more robust compared to clustering coefficient, as it is not influenced by nodes with small number of connections (Newman, 2003).

		Modularity	The extent to which a network is characterised by densely interconnected nodes with relatively few connections between nodes in different modules ("cliques"). It is a reflection of the natural segregation within a network.
		Local efficiency	The local efficiency refers to the global efficiency of the subgraph (i.e. fully connected network not connected to the main graph) formed by the adjacent neighbours of the node.

Table 1. Description of network measures investigated in this study.

Study	Modality	Groups	Findings: LLD vs. Controls
Ajilore et al., 2014 (Ajilore et al., 2014)	3T MRI Grey matter volumes	53 LLD and 73 controls	Higher clustering coefficient and path lengths at trend-levels. Lower glofbal efficiency. No difference in resilience to random failure, more vulnerability to targeted attacks based on nodal influence.
Lim et al., 2013 (Lim et al., 2013)	3T MRI Grey matter volumes	37 LLD and 40 controls	No differences in clustering coefficient, path length, and small-world index. Lower nodal betweenness in the medial orbitofrontal and angular gyrus regions.
Bai et al., 2012 (Bai et al., 2012)	DTI	35 RGD, 38 aMCI, and 30 controls	Both RGD and aMCI showed longer path length and lower global efficiency. No differences between RGD and aMCI.
Charlton et al., 2015 (Charlton et al., 2014)	DTI	28 LLD and 48 controls	No differences in global measures. Higher vulnerability in the right prefrontal cortex; lower centrality in the right temporal region.
Bohr et al., 2013 (Bohr et al., 2013)	Resting-state fMRI	14 LLD and 16 controls	No differences in global measures.
Li et al., 2014 (Li et al., 2014)	Resting-state fMRI	23 LLD, 18 aMCI, 13 LLD + aMCI, and 25 controls	LLD+aMCI showed longer path length and lower global efficiency. Both LLD groups showed lower local efficiency.

Table 2. Literature summary of principal findings in network studies in LLD across imaging modalities. Abbreviations: LLD = Late-life depression; MRI = Magnetic Resonance Imaging; DTI = Diffusion tensor imaging; RGD = remitted geriatric depression; aMCI = amnestic mild cognitive impairment.

	Controls	LLD	p value
n	25	33	
Age (yrs)	73.6 ± 6.0	73.6 ± 5.2	0.96[t]
Age range	61 – 80	60 – 84	
Gender (male, %)	7 (28%)	8 (24.24%)	0.75[§]
Disease duration (months)		22.6 ± 20.7	NA
Onset (years)		51.0 ± 22.1	NA
MMSE	29.6 ± 0.8	28.9 ± 1.0	0.01[w]
MADRS		13.5 ± 10.9	NA
GDS		12.4 ± 8.1	NA
CIRS-G	3.6 ± 1.5	6.4 ± 2.6	<0.001[t]
Mean cortical thickness (mm)	2.29 ± 0.08	2.26 ± 0.13	0.34[a]
Total WMH (mL)	10.3 ± 15.5	8.4 ± 8.3	0.73[a]
Pv WMH (mL)	6.7 ± 7.8	6.1 ± 5.5	0.99[a]
Deep WMH (mL)	3.6 ± 8.7	2.2 ± 3.4	0.53[a]

Table 3. Values expressed as Mean ± SD.
T= Student's T-Test; [w] = Wilcoxon Ranksum; [§] = Chi Square Test; [a] ANOVA, WMH = white matter hyperintensities; Pv WMH = periventricular WMH; MMSE = Mini-mental state examination; MADRS = Montogomery-Asberg depression rating scale; GDS = Geriatric depression scale; CIRS-G = Cumulative illness rating scale for geriatrics. Significance set at $p < 0.05$.

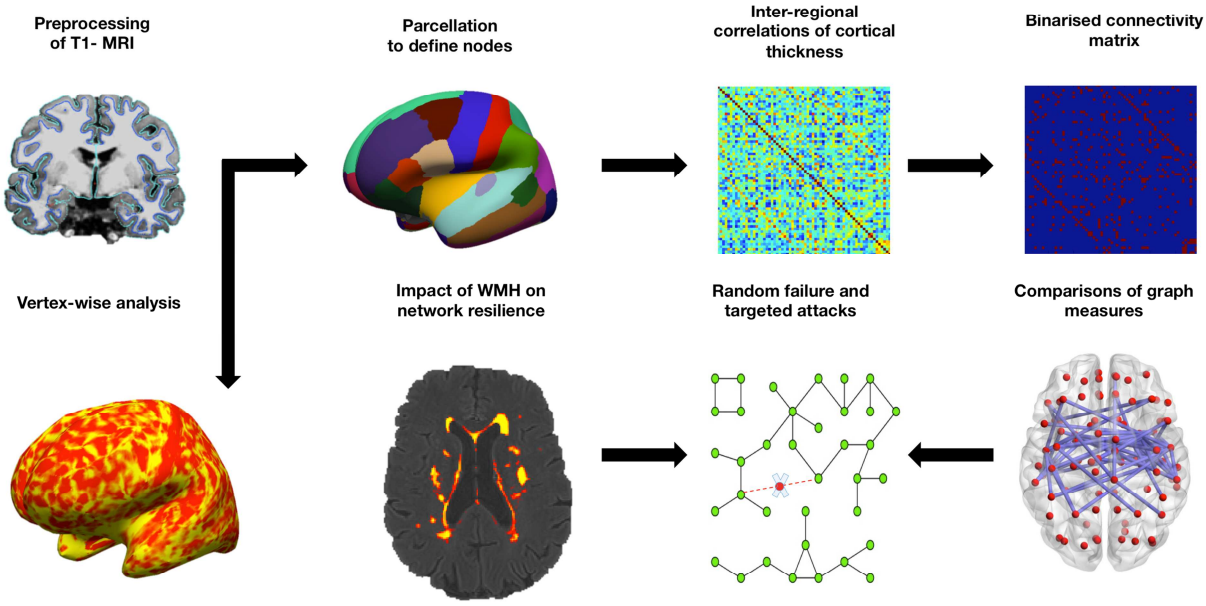

Figure 1. Analytical pipeline. Cortical reconstruction is processed on T1-weighted MRI with Freesurfer for two analytical streams: vertex-wise comparisons of cortical thickness maps between LLD and controls. For the network analyses, brain regions are assigned nodes according to definitions from the Desikan-Killiany parcellation scheme to yield the 68 x 68 association matrix. The inter-regional cortical thickness correlations are thresholded into a binary network containing only the strongest associations. Graph measures are calculated in GAT toolbox for statistical comparisons of network measures between LLD and controls. Resilience of the network was tested with random failures and targeted attacks (i.e. node removal based on betweenness centrality). The potential involvement of WMH on network resilience was investigated by including WMH volumes as an additional nuisance covariate in the resilience analyses. Abbreviations: LLD = Late-life depression; GAT = Graph Analytical Toolbox; WMH = white matter hyperintensities.

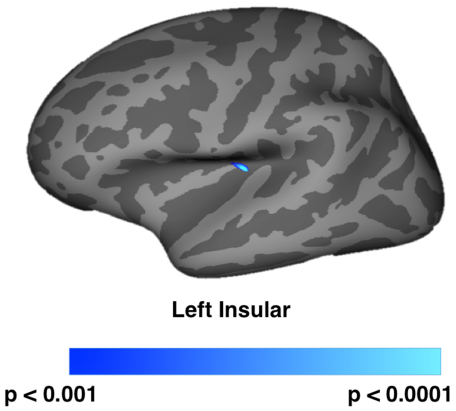

Figure 2. Vertex-wise comparisons of cortical thickness between LLD and Controls. After correcting for age, gender and CIRS-G, cortical thickness was lower was observed in the left insular of the LLD compared to controls at $p < 0.001$ (uncorrected for multiple comparisons). Abbreviations: LLD = Late life depression; CIRS-G = Cumulative illness rating scale for geriatrics.

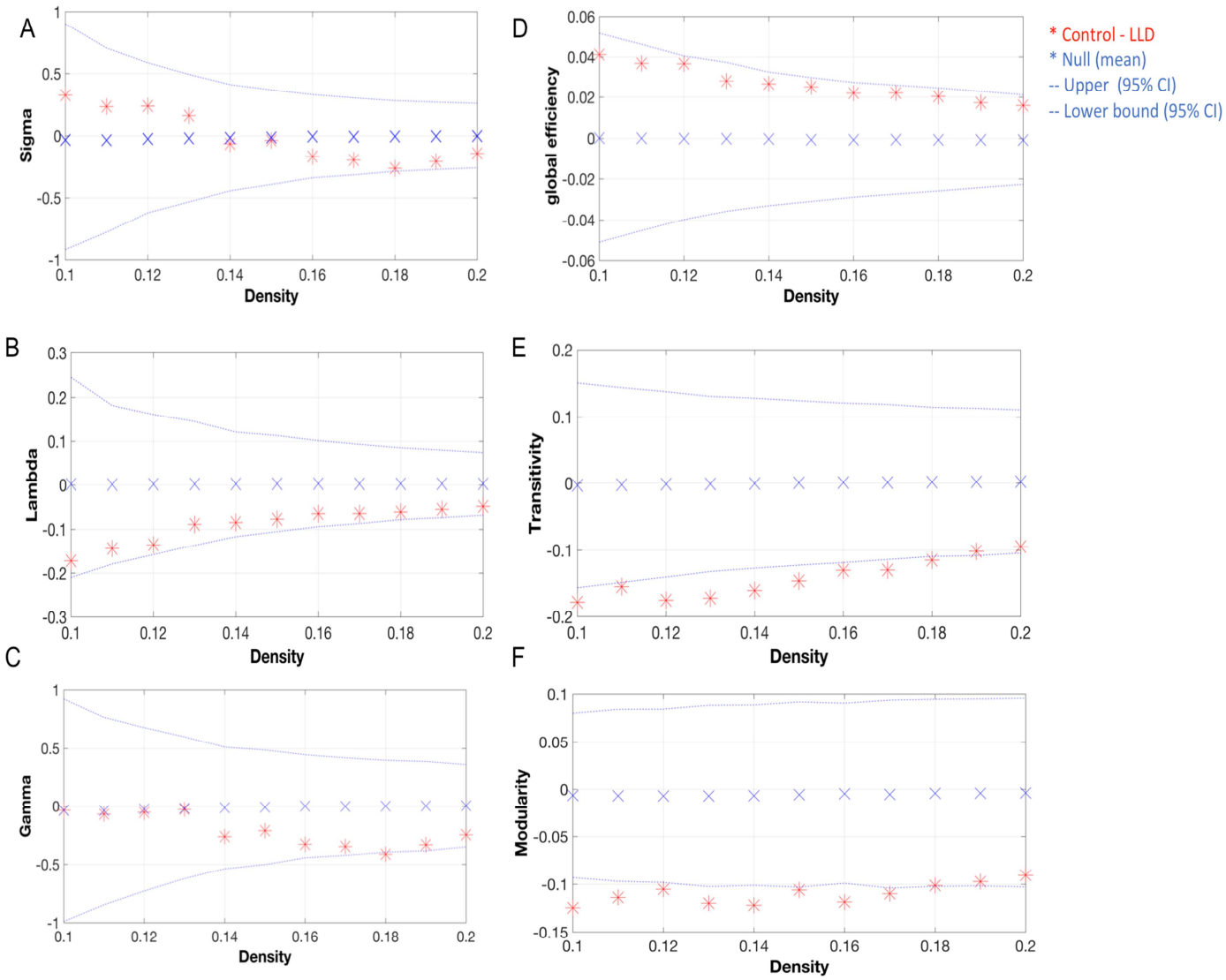

Figure 3. Between-group differences in global network topology as a function of network density. (A) Small-world index **(B)** Lambda (normalized characteristic path length) **(C)** Gamma (normalized clustering coefficient), **(D)** clustering coefficient **(E)** transitivity coefficient **(F)** modularity. The red * marker represents the difference between LLD and controls network (+ve = Controls > LLD; -ve = LLD > Controls), with those positioned out of the confidence intervals representing significant differences after permutation testing with 1000 repetitions ($p < 0.05$). Abbreviations: LLD = Late-life depression.

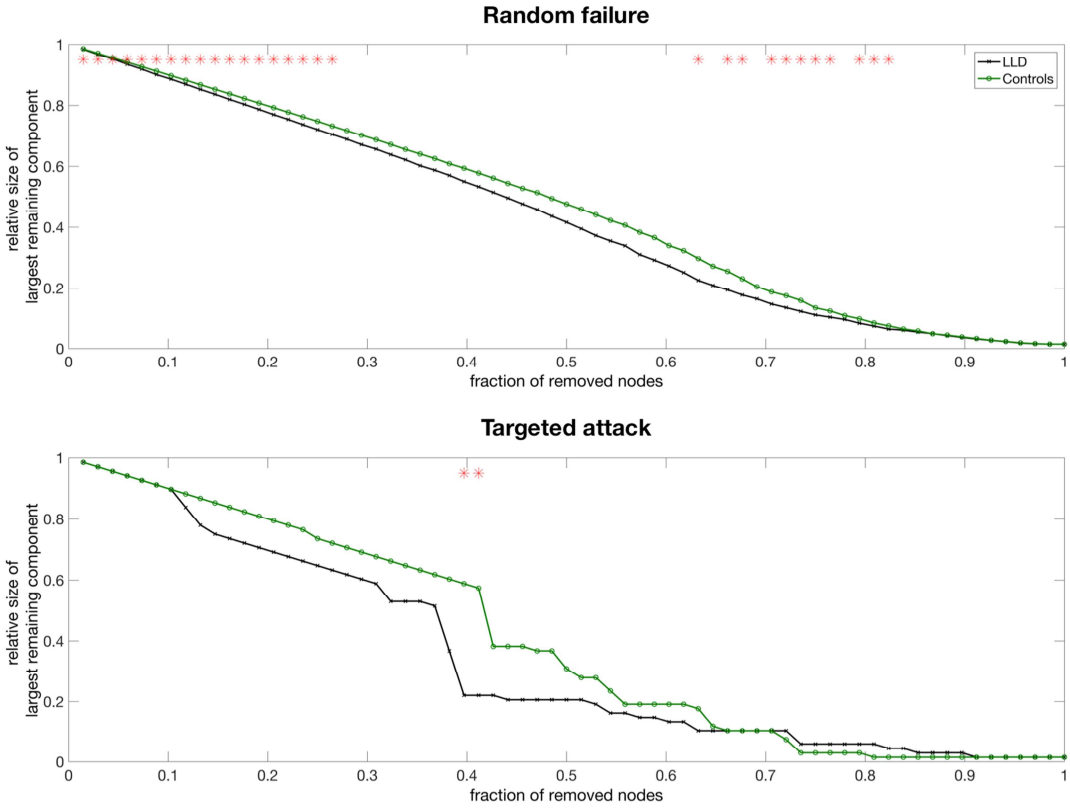

Figure 4. Comparison of network resilience. Changes in the size of the largest component of the remaining network after **(A)** cascading random failure and **(B)** targeted attack in order of nodal betweenness. The red * marker significant differences in the size of the largest remaining component between LLD and controls. Abbreviations: LLD = Late-life depression.

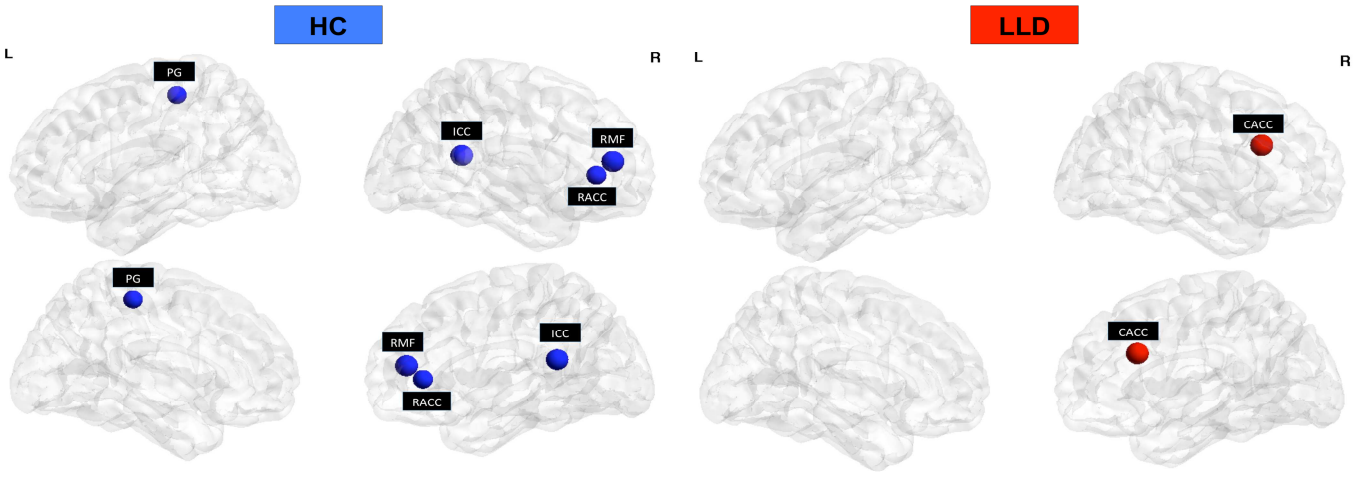

Figure 5. Spatial distribution of hubs in the structural covariance networks of controls and LLD. Abbreviations: PG = Paracentral gyrus, **ICC** = isthmus cingulate cortex, **RMF** = right rostral middle frontal cortex, **RACC** = rostral anterior cingulate cortex, **CACC** = caudal anterior cingulate cortex.

REFERENCES

Achard, S., Salvador, R., Whitcher, B., Suckling, J., Bullmore, E., 2006. A resilient, low-frequency, small-world human brain functional network with highly connected association cortical hubs. J. Neurosci. 26, 63–72. doi:10.1523/JNEUROSCI.3874-05.2006

Ajilore, O., Lamar, M., Leow, A., Zhang, A., Yang, S., Kumar, A., 2014. Graph Theory Analysis of Cortical-Subcortical Networks in Late-Life Depression. Am. J. Geriatr. Psychiatry 22, 195–206. doi:10.1016/j.jagp.2013.03.005

Alexander-Bloch, A., Giedd, J.N., Bullmore, E., 2013. Imaging structural co-variance between human brain regions. Nat. Rev. Neurosci. 14, 322–36. doi:10.1038/nrn3465

Awata, S., Ito, H., Konno, M., Ono, S., Kawashima, R., Fukuda, H., Sato, M., 1998. Regional cerebral blood flow abnormalities in late-life depression: relation to refractoriness and chronification. Psychiatry Clin Neurosci 52, 97–105. doi:10.1111/j.1440-1819.1998.tb00980.x

Bai, F., Shu, N., Yuan, Y., Shi, Y., Yu, H., Wu, D., Wang, J., Xia, M., He, Y., Zhang, Z., 2012. Topologically Convergent and Divergent Structural Connectivity Patterns between Patients with Remitted Geriatric Depression and Amnestic Mild Cognitive Impairment. J. Neurosci. 32, 4307–4318. doi:10.1523/JNEUROSCI.5061-11.2012

Ballmaier, M., Sowell, E.R., Thompson, P.M., Kumar, A., Narr, K.L., Lavretsky, H., Welcome, S.E., DeLuca, H., Toga, A.W., 2004. Mapping brain size and cortical gray matter changes in elderly depression. Biol. Psychiatry 55, 382–389. doi:10.1016/j.biopsych.2003.09.004

Bassett, D.S., Bullmore, E., Verchinski, B. a, Mattay, V.S., Weinberger, D.R., Meyer-Lindenberg, A., 2008. Hierarchical organization of human cortical networks in health and schizophrenia. J. Neurosci. 28, 9239–9248. doi:10.1523/JNEUROSCI.1929-08.2008

Bernhardt, B.C., Chen, Z., He, Y., Evans, A.C., Bernasconi, N., 2011. Graph-theoretical analysis reveals disrupted small-world organization of cortical thickness correlation networks in temporal lobe epilepsy. Cereb. Cortex 21, 2147–2157. doi:10.1093/cercor/bhq291

Bohr, I.J., Kenny, E., Blamire, A., O'Brien, J.T., Thomas, A.J., Richardson, J., Kaiser, M., 2013. Resting-State Functional Connectivity in Late-Life Depression: Higher Global Connectivity and More Long Distance Connections. Front. Psychiatry 3, 1–14. doi:10.3389/fpsyt.2012.00116

Bullmore, E., Sporns, O., 2009. Complex brain networks: graph theoretical analysis of structural and functional systems. Nat. Rev. Neurosci. 10, 186–98. doi:10.1038/nrn2575

Charlton, R.A., Leow, A., GadElkarim, J., Zhang, A., Ajilore, O., Yang, S., Lamar, M., Kumar, A., 2014. Brain Connectivity in Late-Life Depression and Aging Revealed by Network Analysis. Am. J. Geriatr. Psychiatry 23, 642–650. doi:10.1016/j.jagp.2014.07.008

Colloby, S.J., Firbank, M.J., Thomas, A.J., Vasudev, A., Parry, S.W., O'Brien, J.T., 2011a. White matter changes in late-life depression: A diffusion tensor imaging study. J. Affect. Disord. 135, 216–220. doi:10.1016/j.jad.2011.07.025

Colloby, S.J., Firbank, M.J., Vasudev, A., Parry, S.W., Thomas, A.J., O'Brien, J.T., 2011b. Cortical thickness and VBM-DARTEL in late-life depression. J. Affect. Disord. 133, 158–164. doi:10.1016/j.jad.2011.04.010

Colloby, S.J., Vasudev, A., O'Brien, J.T., Firbank, M.J., Parry, S.W., Thomas, A.J., 2011c. Relationship of orthostatic blood pressure to white matter hyperintensities and subcortical volumes in late-life depression. Br. J. Psychiatry 199, 404–410.

doi:10.1192/bjp.bp.110.090423

Crossley, N. a., Mechelli, A., Scott, J., Carletti, F., Fox, P.T., Mcguire, P., Bullmore, E.T., 2014. The hubs of the human connectome are generally implicated in the anatomy of brain disorders. Brain 137, 2382–2395. doi:10.1093/brain/awu132

Dai, Z., He, Y., 2014. Disrupted structural and functional brain connectomes in mild cognitive impairment and Alzheimer's disease. Neurosci. Bull. 30, 217–232. doi:10.1007/s12264-013-1421-0

Daianu, M., Jahanshad, N., Nir, T.M., Jack, C.R., Weiner, M.W., Bernstein, M. a., Thompson, P.M., 2015. Rich club analysis in the Alzheimer's disease connectome reveals a relatively undisturbed structural core network. Hum. Brain Mapp. 3103, n/a–n/a. doi:10.1002/hbm.22830

de Haan, W., Pijnenburg, Y. a L., Strijers, R.L.M., van der Made, Y., van der Flier, W.M., Scheltens, P., Stam, C.J., 2009. Functional neural network analysis in frontotemporal dementia and Alzheimer's disease using EEG and graph theory. BMC Neurosci. 10, 101. doi:10.1186/1471-2202-10-101

Desikan, R.S., Ségonne, F., Fischl, B., Quinn, B.T., Dickerson, B.C., Blacker, D., Buckner, R.L., Dale, A.M., Maguire, R.P., Hyman, B.T., Albert, M.S., Killiany, R.J., 2006. An automated labeling system for subdividing the human cerebral cortex on MRI scans into gyral based regions of interest. Neuroimage 31, 968–980. doi:10.1016/j.neuroimage.2006.01.021

Fischl, B., Dale, A.M., 2000. Measuring the thickness of the human cerebral cortex from magnetic resonance images. Proc Natl Acad Sci U S A 97, 11050–11055. doi:10.1073/pnas.200033797

Fischl, B., Sereno, M.I., Dale, A.M., 1999. Cortical surface-based analysis. II: Inflation, flattening, and a surface-based coordinate system. Neuroimage 9, 195–207. doi:10.1006/nimg.1998.0396

Gong, G., He, Y., Chen, Z.J., Evans, A.C., 2012. Convergence and divergence of thickness correlations with diffusion connections across the human cerebral cortex. Neuroimage 59, 1239–1248. doi:10.1016/j.neuroimage.2011.08.017

Hagmann, P., Cammoun, L., Gigandet, X., Meuli, R., Honey, C.J., Van Wedeen, J., Sporns, O., 2008. Mapping the structural core of human cerebral cortex. PLoS Biol. 6, 1479–1493. doi:10.1371/journal.pbio.0060159

He, Y., Chen, Z., Evans, A., 2008. Structural insights into aberrant topological patterns of large-scale cortical networks in Alzheimer's disease. J. Neurosci. 28, 4756–4766. doi:10.1523/JNEUROSCI.0141-08.2008

He, Y., Chen, Z.J., Evans, A.C., 2007. Small-world anatomical networks in the human brain revealed by cortical thickness from MRI. Cereb. Cortex 17, 2407–2419. doi:10.1093/cercor/bhl149

Herrmann, L.L., Le Masurier, M., Ebmeier, K.P., 2007. White matter hyperintensities in late life depression: a systematic review. J. Neurol. Neurosurg. Psychiatry 79, 619–624. doi:10.1136/jnnp.2007.124651

Hosseini, S.M.H., Hoeft, F., Kesler, S.R., 2012. Gat: A graph-theoretical analysis toolbox for analyzing between-group differences in large-scale structural and functional brain networks. PLoS One 7. doi:10.1371/journal.pone.0040709

Hutton, C., Draganski, B., Ashburner, J., Weiskopf, N., 2009. A comparison between voxel-based cortical thickness and voxel-based morphometry in normal aging. Neuroimage 48, 371–380. doi:http://dx.doi.org/10.1016/j.neuroimage.2009.06.043

Joyce, K.E., Hayasaka, S., Laurienti, P.J., 2013. The Human Functional Brain Network Demonstrates Structural and Dynamical Resilience to Targeted Attack. PLoS Comput. Biol. 9, 1–11. doi:10.1371/journal.pcbi.1002885

Kelly, C., Toro, R., Di Martino, A., Cox, C.L., Bellec, P., Castellanos, F.X., Milham, M.P., 2012. A convergent functional architecture of the insula emerges across imaging modalities. Neuroimage 61, 1129–1142. doi:10.1016/j.neuroimage.2012.03.021

Kenny, E.R., O'Brien, J.T., Cousins, D.A., Richardson, J., Thomas, A.J., Firbank, M.J., Blamire, A.M., 2010. Functional connectivity in late-life depression using resting-state functional magnetic resonance imaging. Am. J. Geriatr. Psychiatry 18, 643–51. doi:10.1097/JGP.0b013e3181cabd0e

Koolschijn, P.C.M.P., van Haren, N.E.M., Schnack, H.G., Janssen, J., Hulshoff Pol, H.E., Kahn, R.S., 2010. Cortical thickness and voxel-based morphometry in depressed elderly. Eur. Neuropsychopharmacol. 20, 398–404. doi:10.1016/j.euroneuro.2010.02.010

Li, W., Douglas Ward, B., Liu, X., Chen, G., Jones, J.L., Antuono, P.G., Li, S.-J., Goveas, J.S., 2014. Disrupted small world topology and modular organisation of functional networks in late-life depression with and without amnestic mild cognitive impairment. J. Neurol. Neurosurg. Psychiatry 1–9. doi:10.1136/jnnp-2014-309180

Lim, H.K., Jung, W.S., Aizenstein, H.J., 2013. Aberrant topographical organization in gray matter structural network in late life depression: a graph theoretical analysis. Int. Psychogeriatrics 25, 1929–1940. doi:10.1017/S104161021300149X

Meltzer, C.C., Smith, G., DeKosky, S.T., Pollock, B.G., Mathis, C.A., Moore, R.Y., Kupfer, D.J., Reynolds, C.F., 1998. Serotonin in aging, late-life depression, and Alzheimer's disease: the emerging role of functional imaging. Neuropsychopharmacology 18, 407–30. doi:10.1016/S0893-133X(97)00194-2

Montgomery, S.A., Asberg, M., 1979. A new depression scale designed to be sensitive to change. Br. J. Psychiatry 134, 382–9.

Naismith, S.L., Norrie, L.M., Mowszowski, L., Hickie, I.B., 2012. The neurobiology of depression in later-life: Clinical, neuropsychological, neuroimaging and pathophysiological features. Prog. Neurobiol. 98, 99–143. doi:10.1016/j.pneurobio.2012.05.009

Nascimento, K.K.F. do, Silva, K.P., Malloy-Diniz, L.F., Butters, M.A., Diniz, B.S., 2015. Plasma and cerebrospinal fluid amyloid-β levels in late-life depression: A systematic review and meta-analysis. J. Psychiatr. Res. 69, 35–41. doi:10.1016/j.jpsychires.2015.07.024

Newman, M.E.J., 2003. The structure and function of complex networks. SIAM Rev. 45(2), 167–256. doi:10.1137/S003614450342480

Rubinov, M., Sporns, O., 2010. Complex network measures of brain connectivity: Uses and interpretations. Neuroimage 52, 1059–1069. doi:10.1016/j.neuroimage.2009.10.003

Sexton, C.E., Allan, C.L., Masurier, M. Le, Bradley, K.M., Mackay, C.E., Ebmeier, K.P., 2015. Magnetic Resonance Imaging in Late-Life Depression 69, 680–689.

Sexton, C.E., Mackay, C.E., Ebmeier, K.P., 2013. A systematic review and meta-analysis of magnetic resonance imaging studies in late-life depression. Am. J. Geriatr. Psychiatry 21, 184–95. doi:10.1016/j.jagp.2012.10.019

Singh, M.K., Kesler, S.R., Hadi Hosseini, S.M., Kelley, R.G., Amatya, D., Hamilton, J.P., Chen, M.C., Gotlib, I.H., 2013. Anomalous gray matter structural networks in major depressive

disorder. Biol. Psychiatry 74, 777–785. doi:10.1016/j.biopsych.2013.03.005

Sporns, O., Tononi, G., Kötter, R., 2005. The human connectome: A structural description of the human brain. PLoS Comput. Biol. 1, 0245–0251. doi:10.1371/journal.pcbi.0010042

Stam, C.J., De Haan, W., Daffertshofer, a., Jones, B.F., Manshanden, I., Van Cappellen Van Walsum, a. M., Montez, T., Verbunt, J.P. a, De Munck, J.C., Van Dijk, B.W., Berendse, H.W., Scheltens, P., 2009. Graph theoretical analysis of magnetoencephalographic functional connectivity in Alzheimer's disease. Brain 132, 213–224. doi:10.1093/brain/awn262

Supekar, K., Menon, V., Rubin, D., Musen, M., Greicius, M.D., 2008. Network analysis of intrinsic functional brain connectivity in Alzheimer's disease. PLoS Comput. Biol. 4. doi:10.1371/journal.pcbi.1000100

Thomas, A.J., Ferrier, I.N., Kalaria, R.N., Perry, R.H., Brown, A., O'Brien, J.T., 2001. A neuropathological study of vascular factors in late-life depression. J Neurol Neurosurg Psychiatry 70, 83–7. doi:10.1136/jnnp.70.1.83

Tsopelas, C., Stewart, R., Savva, G.M., Brayne, C., Ince, P., Thomas, A., Matthews, F.E., 2011. Neuropathological correlates of late-life depression in older people. Br. J. Psychiatry 198, 109–14. doi:10.1192/bjp.bp.110.078816

Váša, F., Shanahan, M., Hellyer, P.J., Scott, G., Cabral, J., Leech, R., 2015. Effects of lesions on synchrony and metastability in cortical networks. Neuroimage. doi:10.1016/j.neuroimage.2015.05.042

Yao, Z., Zhang, Y., Lin, L., Zhou, Y., Xu, C., Jiang, T., 2010. Abnormal cortical networks in mild cognitive impairment and alzheimer's disease. PLoS Comput. Biol. 6. doi:10.1371/journal.pcbi.1001006

Yesavage, J.A., Brink, T.L., Rose, T.L., Lum, O., Huang, V., Adey, M., Leirer, V.O., 1982. Development and validation of a geriatric depression screening scale: a preliminary report. J Psychiatr Res 17, 37–49.

HIGHLIGHTS

- We performed a multi-modal study assessing cortical thickness and structural covariance in late-life depression (LLD).
- No significant reduction of cortical thickness was found in LLD and controls.
- However, the LLD network was more segregated (i.e. greater transitivity and modularity).
- White matter lesions might undermine the topological stability of the LLD network.

VERIFICATION

ACKNOWLEDGEMENTS

This work was supported by the NIHR Biomedical Research Unit in Dementia and the Biomedical Research Centre awarded to Cambridge University Hospitals NHS Foundation Trust and the University of Cambridge, and the NIHR Biomedical Research Unit in Dementia and the Biomedical Research Centre awarded to Newcastle upon Tyne Hospitals NHS Foundation Trust and the Newcastle University. Elijah Mak was in receipt of a Gates Cambridge, PhD studentship.

FINANCIAL DISCLOSURES

Elijah Mak has no competing interests.

Sean Colloby has no competing interests.

Alan Thomas reports grants from the Medical Research Council, NIHR, ARUK and the Alzheimer's Society and has received funding from GE Healthcare for investigator led research

John O'Brien reports grants from the Medical Research Council, NIHR, ARUK and the Alzheimer's Society and has acted as a consultant for GE Healthcare, Lilly, TauRx, Axona and Cytox.

DATA

All authors have complete access to the data. This manuscript has not been published or is currently under review elsewhere.